ADVANCED MATERIALS INTERFACES
Open Access
www.advmatinterfaces.de

Understanding Hydration in CPO-27 Metal-Organic Frameworks: Strong Impact of the Chemical Nature of the Metal (Cu, Zn)

Marvin Kloß, Michael Beerbaum, Dominik Baier, Christian Weinberger, Frederik Zysk, Hossam Elgabarty, Thomas D. Kühne, and Michael Tiemann**

CPO-27 is a metal-organic framework (MOF) with coordinatively unsaturated metal centers (open metal sites). It is therefore an ideal host material for small guest molecules, including water. This opens up numerous possible applications, such as proton conduction, humidity sensing, water harvesting, or adsorption-driven heat pumps. For all of these applications, profound knowledge of the adsorption and desorption of water in the micropores is mandatory. The hydration and water structure in CPO-27-*M* (*M* = Zn or Cu) is investigated using water vapor sorption, Fourier transform infrared (FTIR) spectroscopy, density functional theory (DFT) calculations, and molecular dynamics simulation. In the pores of CPO-27-Zn, water binds as a ligand to the Zn center. Additional water molecules are stepwise incorporated at defined positions, forming a network of H-bonds with the framework and with each other. In CPO-27-Cu, hydration proceeds by an entirely different mechanism. Here, water does not coordinate to the metal center, but only forms H-bonds with the framework; pore filling occurs mostly in a single step, with the open metal site remaining unoccupied. Water in the pores forms clusters with extensive intra-cluster H-bonding.

1. Introduction

Within the constantly growing diversity of metal-organic frameworks (MOFs),[1,2] materials with open metal sites, that is coordinatively unsaturated metal centers, are particularly interesting.[3] One fascinating example is CPO-27,[4] also known as MOF-74.[5] It contains the linker ligand 2,5-dioxido-1,4-benzenedicarboxylate ($dobdc^{4-}$) and has been synthesized using a large number of metals, including Zn[5] and Cu.[6] CPO-27 has 1D micropores arranged in parallel with a honeycomb-like cross section. The metal centers are coordinated by three carboxylate and two phenolate groups of the linker molecules, as well as by a solvent molecule from the synthesis (dimethylformamide (DMF) or water). Removal of this molecule through thermal activation creates the open metal site that is exposed to (and therefore accessible through) the pores. Thus, a variety of guest molecules, including H_2O, can coordinate to the open metal sites.[7-9] Numerous applications are based on the uptake of water, such as humidity sensing,[10,11] water harvesting,[12,13] proton conduction,[14-18] or adsorption-driven heat pumps.[19] Other applications aim at the uptake of other molecules, for example, gas sensing (other than water),[20,21] carbon capture,[22,23] or catalysis.[24] In these latter cases, water can be an interfering component that competes with the target molecule for sorption sites. In addition, the structural integrity of the framework materials may be affected by humidity.[25] Hence, it is mandatory to understand the behavior of water inside the pores of the CPO-27 host material.

CPO-27 may be regarded as an ideal system for comprehensive hydration/dehydration studies, because intra-pore water molecules are known to occupy well-defined sites. Dietzel *et al.*

M. Kloß, D. Baier, C. Weinberger, M. Tiemann
Department of Chemistry – Inorganic Chemistry
Faculty of Science
Paderborn University
Warburger Str. 100, 33098 Paderborn, Germany
E-mail: michael.tiemann@upb.de

The ORCID identification number(s) for the author(s) of this article can be found under https://doi.org/10.1002/admi.202400476

DOI: 10.1002/admi.202400476

M. Beerbaum, T. D. Kühne
Center for Advanced Systems Understanding (CASUS)
Untermarkt 20, 02826 Görlitz, Germany
E-mail: t.kuehne@hzdr.de
M. Beerbaum, T. D. Kühne
Helmholtz Zentrum Dresden-Rossendorf
Bautzner Landstr. 400, 01328 Dresden, Germany
F. Zysk, H. Elgabarty
Department of Chemistry – Theoretical Chemistry
Faculty of Science
Paderborn University
Warburger Str. 100, 33098 Paderborn, Germany

identified five crystallographically defined water molecules per Zn center in fully hydrated CPO-27-Zn.[25] Based on temperature-dependent, in situ powder X-ray diffraction (XRD) and thermal analysis data, they categorized the five molecules in three distinct groups, according to their strength of interaction with the host material and with neighboring water molecules:[9] (i) The water molecule that coordinates to the metal center exhibits the strongest adsorption strength (chemisorption). (ii) Two more molecules interact with the coordinating one by H-bonding and show a weaker adsorption strength. (iii) Finally, the last two water molecules interact only with the last-mentioned two molecules by H-bonding and exhibit the weakest adsorption strength. The formula of CPO-27-Zn is therefore $[Zn_2(dobdc)(H_2O)_2]\cdot 8H_2O$, indicating that two water molecules (one per Zn) coordinate, while eight molecules (four per Zn) are considered as crystal water molecules inside the pores.

Obviously, measuring the adsorption (and desorption) of water from the gas phase is a very promising means of studying the hydration (and dehydration) behavior of MOFs.[26,27] However, for CPO-27, water sorption studies to date have mostly employed the gravimetric method (microbalance), with particular focus on the structural integrity of the framework.[28,29] The manometric technique, on the other hand, has proven to be a very powerful means of studying water vapor sorption in many porous media including some MOFs;[30,31] however, to the best of our knowledge, it has not been applied systematically to CPO-27. The manometric technique provides very high accuracy especially for very low amounts of water, that is, low water vapor pressure. This is particularly helpful for detailed hydration/dehydration studies in CPO-27, due to the strong water-metal interaction.

Further insight in the unique behavior of water in confined space is obtained by computational methods. Density functional theory (DFT) has been applied to CPO-27-*M* (*M* = Cu, Mg, Zn) to study adsorption energies and preferred adsorption sites of small molecules (*e.g.* CO_2,[32,33] N_2,[32,33] and H_2[32,34]). Studies focusing on the adsorption of water in CPO-27-*M* (*M* = Mg, Zn)[35,36] outline differences between the first (open metal site), second (near the oxygen atoms of the inorganic building units) and third water sorption sites (near the phenylene backbone). While results on CPO-27-Zn[35] strongly suggest an energetically favorable adsorption to the first site, simulations for CPO-27-Mg[36,37] suggest otherwise. In the latter, similar sorption energies for the first two sorption sites, after adsorption of one water molecule, suggest a simultaneous occupancy of both positions, while the third sorption site is far less attractive. Depending on the metal center, these observations hint toward a different sorption process.

Here we present a study on the hydration behavior and water structure in CPO-27-Zn and CPO-27-Cu by a combined experimental and computational approach. The objectives of our investigation is to gain a better understanding of the interactions between water molecules and the framework (coordinative bonding, hydrogen bonds) on the one hand, and the H-bonding behavior of the water molecules among themselves on the other hand. In particular, water-induced structural changes in the framework are investigated. We study the adsorption and desorption of water by manometric vapor sorption analysis. In addition, water-induced structural distortion and changes in charge distribution of the materials are discussed by employing density functional theory (DFT). The DDEC6 atomic population analysis[38–43] obtains net atomic charges (NAC) by assigning valence electrons as a function of the total electron density distribution to the observed system. The obtained NAC are calculated on several criteria, such as transferability to different conformations of the same molecules. The electron density distribution needed for the analysis is obtained by DFT. Further, the spatial distribution of water molecules in the pores is analyzed using semi-empirical (PM6-FM) molecular dynamics (MD) simulations. Combination of static and dynamic calculations allows for a unique insight, understanding the differences in macroscopic behavior on an atomic levels.

2. Results and Discussion

2.1. General Characterization

CPO-27-Zn[44] and CPO-27-Cu[45] were prepared by modified solvothermal methods previously reported in the literature, as described in detail in the Supporting Information section. Powder X-ray diffraction (XRD) patterns (**Figure 1**a/b) confirm the framework structure of all materials with no evidence of crystalline impurities. To assess the stability of the frameworks to an excess of water, the materials were washed with water (approx. 50 mg sample with 8 to 10 mL H_2O) and then air-dried on filter paper at room temperature. XRD confirms that both materials remain crystalline. The microporous nature of the products is confirmed by N_2 physisorption analysis, revealing type-I sorption isotherms (Figure 1c).[46] The measurements prove high surface areas and large pore volumes (Table S1, Supporting Information).

Elemental analysis of the hydrated materials reveals C/H ratios that are reasonably consistent with mostly defect-free frameworks (Table S2, Supporting Information). The calculated number of water molecules per formula unit (M_2(dobdc)) is approximately ten for CPO-27-Zn, in accordance with literature data.[25] CPO-27-Cu-hyd has only 9 water molecules per formula unit, which can be explained by generally weak interaction of the Cu^{2+} open metal site with guest molecules[45,47] due to Jahn-Teller distortion.[48] Thermogravimetric analysis coupled with mass spectrometry (TGA/MS) of the hydrated frameworks reveal very similar results to those obtained by Dietzel *et al.* (Figure S1, Supporting Information).[9]

Fourier transform infrared (FTIR) spectra of the desolvated frameworks (**Figure 2**a) show the absence of the carboxyl O—H vibration, confirming the absence of unreacted (protonated) linker molecules. Spectra of the hydrated samples show typical vibration bands of water (for a closer inspection of the stretching modes, see below). Otherwise, the spectra show only slight differences (slight shifts in the oscillation frequencies) to those of the desolvated materials. In the low wavenumber region (Figure 2b), the M—O stretching vibration within the framework[8,49] is observed at slightly higher wavenumber for CPO-27-Cu (600 cm^{-1}) than for CPO-27-Zn (580 cm^{-1}), suggesting a higher Cu—O than Zn—O bond strength. This is consistent with the observation of shorter distances between the Cu center and the coordinating O atoms in the framework (see below).

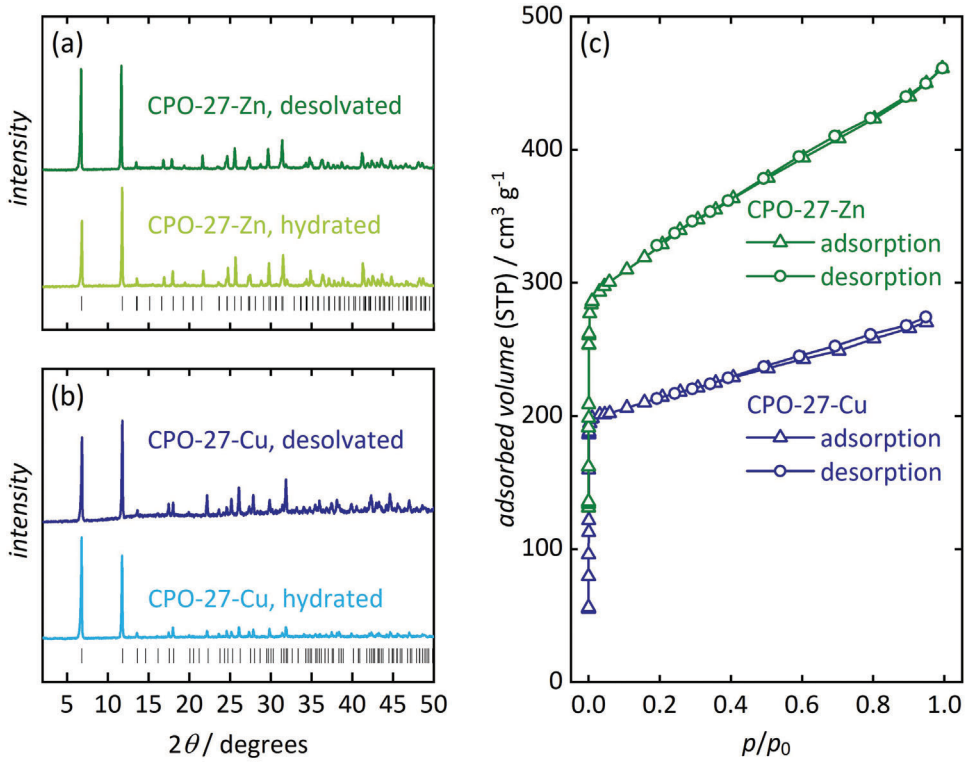

Figure 1. Powder X-ray diffraction patterns of desolvated and hydrated frameworks, (a) CPO-27-Zn and (b) CPO-27-Cu, confirming structural integrity after hydration. (c) N_2 sorption isotherms of CPO-27-Zn and CPO-27-Cu (the latter sample showed extra-pore condensation at the highest measured pressure, $p/p_0 = 0.995$; the respective data point was removed for clarity).

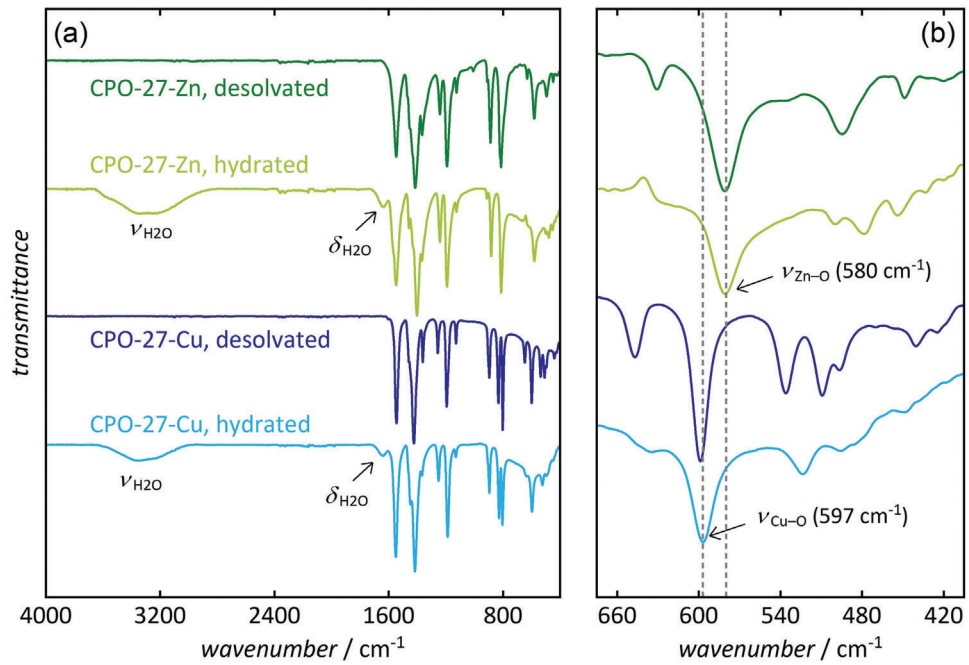

Figure 2. FTIR spectra of desolvated and hydrated CPO-27-Zn and CPO-27-Cu. Hydrated samples show typical H_2O vibration bands (a); the Cu—O stretching vibration occurs at slightly higher wavenumber than Zn—O (b).

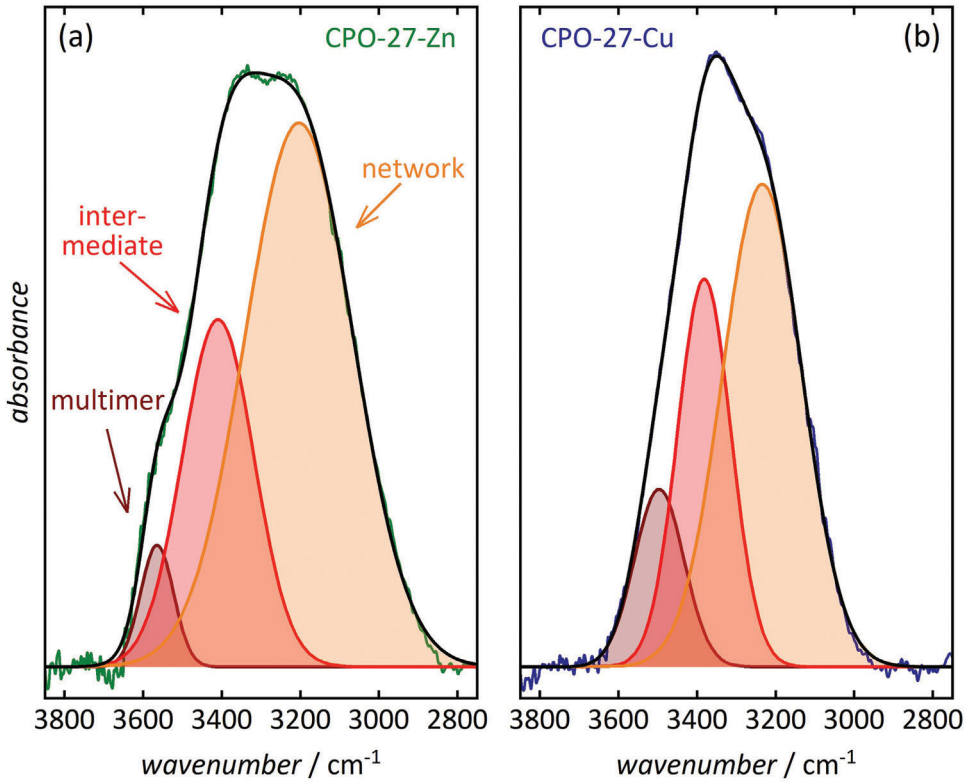

Figure 3. Deconvolution by least-square fitting of the FTIR O–H stretching vibration band of water in hydrated (a) CPO-27-Zn and (b) CPO-27-Cu, revealing a higher degree of H-bonding ('network water') in CPO-27-Zn than in CPO-27-Cu (black lines are the sums of the three fitted Gaussian profiles).

2.2. Experimental Studies of Hydration

A closer inspection of the stretching vibration bands of H_2O in the hydrated samples by FTIR in attenuated total reflection (ATR) mode provides some insight in the interactions of water molecules within the pores. Previous studies have shown that for water in confinement, the O—H stretching vibration band in the range of 2800 ... 3700 cm^{-1} can be deconvoluted into three contributions originating from water in different environments.[30,31,50] Three bands that result from least-square fitting of Gaussian profiles correspond to 'network water' (molecules that interact strongly with adjacent ones by approximately four H-bonds), 'multimer water' (molecules that are poorly connected by only a few H-bonds), and 'intermediate water' (H-bonding situation between 'network' and 'multimer'). **Figure 3** shows that the relative contribution from network water is higher in CPO-27-Zn (71%) than in CPO-27-Cu (55%), while the opposite is observed for the contribution from multimer water (Zn: 5%; Cu: 14%). Hence, water molecules in the pores of CPO-27-Zn seem to form more extensive H-bonding networks than in CPO-27-Cu, as discussed below.

To understand the hydration and dehydration of CPO-27-Zn and CPO-27-Cu in more detail, we carried out manometric water vapor sorption measurements at 25°C. Two consecutive cycles of adsorption/desorption were performed without removing the sample from the device between cycles, that is without additional thermal activation after the first cycle. This allows to identify water molecules that occupy the open sites, that is, coordinate to the metal centers, since these will not be removed by the desorption process. In this case, a different situation is expected for the second adsorption isotherm. For both materials, an overall higher total uptake is observed during the second adsorption/desorption cycle than during the first cycle (see below). We explain this finding by a partial degradation of the frameworks due to cleavage of metal-linker bonds during the time-consuming measurements (several days), leading to the formation of additional open metal sites. This is consistent with previous reports for MOFs with vacant coordination sites, including CPO-27-Mg.[29]

The water sorption isotherms of CPO-27-Zn show a stepwise progression (**Figure 4a**). Since most of the water is adsorbed at low relative pressure ($p/p_0 < 0.1$), we show all isotherms both in a linear and in a semi-logarithmic representation. (Figure 4b/c, Missing data points below *ca.* $p/p_0 = 0.002$, except in the first adsorption isotherms, are due to technical experimental restrictions) Initially, a step around $p/p_0 = 0.01$ is observed in the first adsorption isotherm, during which *ca.* 20% of the total water uptake takes place. This step is not reversible, that is these 20% of water remain in the sample after the completed first adsorption/desorption cycle. We assign this uptake to the coordination of water molecules to the open Zn^{2+} centers (first adsorption site). This is consistent with the above-mentioned findings that the coordinating molecule is one out of five crystallographically defined water molecules in the fully hydrated material.[25] Then, further water adsorption occurs in another three distinguishable steps: First, a well-defined step in the pressure range $p/p_0 = 0.01$ ... 0.025 is observed. During this step, another *ca.*

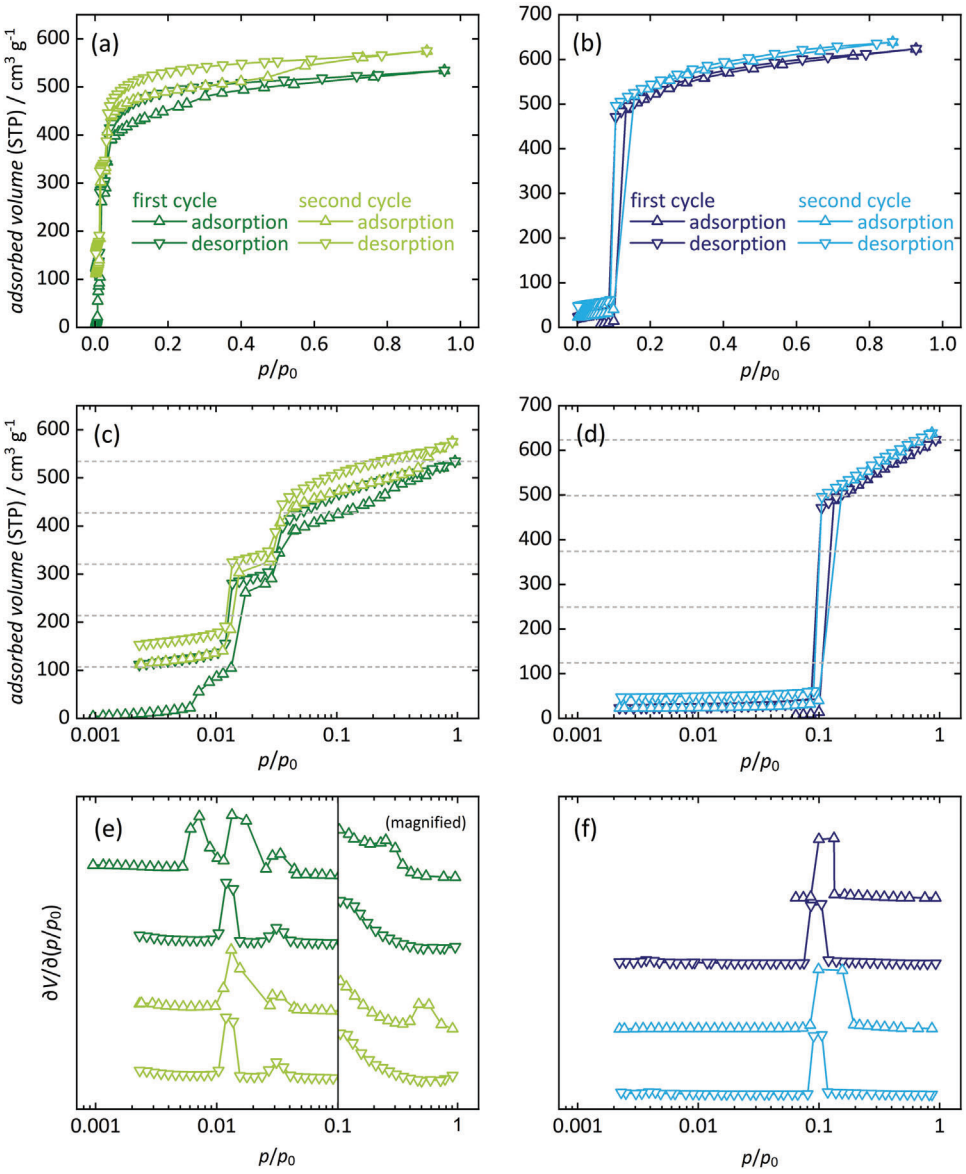

Figure 4. Water vapor sorption isotherms (25°C) of (a) CPO-27-Zn and (b) CPO-27-Cu (two consecutive adsorption/desorption cycles). Data are shown at linear scale, in semi-logarithmic representation (c,d), and as the normalized first derivatives (e,f). Horizontal lines mark 20%, 40%, 60%, 80%, and 100% of the total water uptake during the first cycle.

40% of the total water uptake takes place, which we attribute to two water molecules interacting quite strongly with the coordinating water molecule through H-bonding (second and third adsorption site), consistent with the above-mentioned observations made by Dietzel *et al.*[9] Next, there is another step at p/p_0 = 0.025 ... 0.05, whereby another approx. 20% of the total water uptake occurs (fourth sorption site). This uptake can be attributed to a water molecule with weaker interaction. Finally, the uptake of the remaining *ca.* 20% occurs gradually, over a wide pressure range of p/p_0 = 0.05 ... 1, which corresponds to one last water molecule with the weakest interaction to neighboring molecules.

Both consecutive cycles of adsorption/desorption in CPO-27-Zn show significant hysteresis, which may be interpreted as a configurational rearrangement of the adsorbed water molecules. Hysteresis in water sorption isotherms is often explained by a rearrangement of water molecules (from a metastable state, *i.e.*, preliminary pore saturation) with increasing vapor pressure (*i.e.*, during adsorption). If such a rearrangement leads to an increase in the density of the adsorbed water and is not reversible when the pressure decreases thereafter (*i.e.* during desorption), it will create hysteresis. This effect has been discussed mainly for larger pores and/or for hydrophobic pores (including micropores).[31,51-60] We hypothesize that a similar effect occurs in our case, since the pore walls of CPO-27 contain hydrophobic (phenylene) units between the (hydrophilic) coordinated metal centers. Assuming that all five water molecules are ultimately located at crystallographically defined positions, they may

temporarily (partially) exist in a different, metastable configuration during the adsorption process.

CPO-27-Cu exhibits a completely different water sorption behavior than CPO-27-Zn (Figure 4b). Almost no uptake is observed at pressures up to *ca.* $p/p_0 = 0.1$. Then, adsorption of *ca.* 80% (*i.e.*, four molecules per Cu) occurs all at once, followed by the residual 20% (one molecule) in the remaining pressure range ($p/p_0 = 0.1 \ldots 1$). This behavior resembles classical pore condensation, with no option to distinguish between crystallographically distinct water sites. Almost no hysteresis is observed. Most notably, the adsorption of all five water molecules is reversible, that is, any water molecule near the open site at the Cu^{2+} center, binds only weakly, if at all (see below). This is in accordance with literature data that revealed weak interactions of H_2O with Cu^{2+} centers in other open-metal-site frameworks due to Jahn-Teller distortion.[61] This leads to steric constraints that result in drastically reduced Cu–O Coulomb interactions and significantly lower partial charge than for the other members of the isoreticular series.[34] As a consequence, one oxygen atom of the linker molecule is oriented into the pore, sterically blocking the metal site and inhibiting interactions with water, as will be confirmed by DFT calculation shown below. Ultimately, this oxygen atom acts as a nucleation site facilitating water cluster growth through hydrogen bonding.

Summarizing the water sorption data, we can conclude that the high water uptake at low relative pressure ($p/p_0 < 0.1$) is clear evidence of the hydrophilic nature of CPO-27-Zn. The affinity of the open metal site becomes evident by the coordination of water (strong bonding; 20% of total water uptake). The irreversibility of this sorption process verifies the existence of vacant coordination sites prior to sorption measurements (*i.e.* after activation). Deviating from this behavior, CPO-27-Cu shows a (nearly) reversible pore condensation behavior driven by water-water interactions. Distortion of the local coordination environment causes one oxygen atom from the inorganic building unit to be oriented into the pore, thereby initiating water cluster formation via hydrogen bonding without participation of the Cu^{2+} site (see theoretical calculations below).

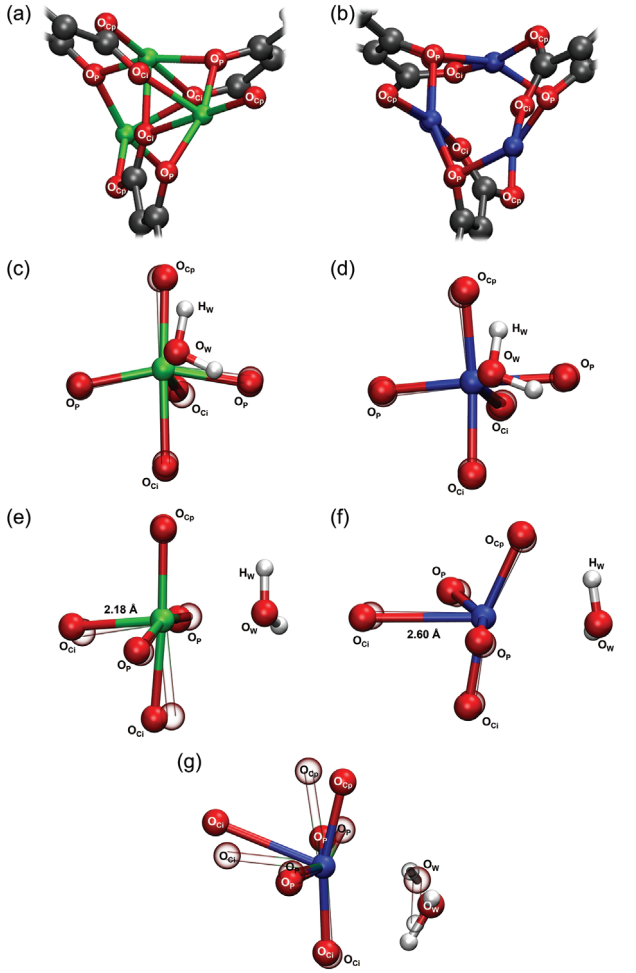

Figure 5. Distinguishable framework O atoms in hydrated (a) CPO-27-Zn and (b) CPO-27-Cu, not showing coordinating water molecules for clarity. Top views (c,d) and side-on views (e,f) of the changes in the local coordination environment before (transparent atoms/bonds) and after (colored atoms/bonds) hydration and geometric optimization. (g) Comparison of the coordination environment in hydrated CPO-27-Cu (solid color) and CPO-27-Zn (hollow). (Color code: O - red, C - dark gray, Zn - green, H - white).

2.3. Computational Studies

DFT simulation of the hydration utilizes supercells of the frameworks ($1 \times 1 \times 4$) under periodic boundary conditions (pbc); the studied structures possess a total of three independent pores with no defects. The supercells are based on crystallographic data of the dehydrated frameworks, that is with unoccupied, open metal sites (M_2(dobdc)).[47] We distinguish three types of framework oxygen atoms (O_{MOF}) according to their respective environment: (i) carboxylate oxygen atoms exposed to the pore (O_{Cp}), (ii) carboxylate oxygen atoms pointing "inward", that is slightly away from the pore (O_{Ci}), and (iii) phenolate oxygen atoms (O_P), as displayed in **Figure** 5a/b. One water molecule was placed next to each metal site at a distance of 2 Å, resulting in the monohydrate framework (M_2(dobdc)(H_2O)$_2$, that is, one water molecule per metal center). The system was then allowed to relax into the geometrically optimized structure. Higher hydration degrees were obtained by filling the pores of less hydrated frameworks with bulk water from centroid molecular dynamics (cmd) simulations using the second-generation Car-Parinello-based quantum ring polymer contraction method, as described in the Supporting Information section.

For CPO-27-Zn, we observe that the water molecule forms a coordinative bond (Figure 5c/d) to the metal. Its oxygen atom O_{water} is at a distance to the Zn center of 2.32 Å (0.2 Å farther than in the hexaaqua zinc(II) complex[62]); its hydrogen atoms H_{water} are in proximity to one O_P and one O_{Cp} atom. This results in a distorted octahedral coordination geometry with most bonds being slightly elongated (see Table S3, Supporting Information). Seven O_{MOF}–H_{water} distances are below 3.0 Å, which indicates a strong affinity of the Zn site to water, in agreement with the water sorption data (Figure 4) and with previous studies.[35]

In addition, the coordination of water causes a change in the electron densities within the framework, which we quantify using the DDEC6 atomic population analysis charges

(see Table S4, Supporting Information). Compared to the (original) desolvated structure, the charge of the O_{Cp} atoms is now significantly higher (−0.526 before → −0.560 after hydration). The same effect, though to a weaker extent, is observed for the O_P atoms (−0.603 → −0.610), while the O_{Ci} atoms are now slightly less negatively charged (−0.592 → −0.585). The Zn center is now slightly more positively charged (+0.977 → +0.987). The changes in electron densities result from both polarization and charge transfer effects due to the presence of the water molecule itself, and also from the subsequently induced geometrical relaxation of the framework, as shown in Table S4 (Supporting Information); the charge increases to +1.000 upon relaxation only, excluding the influence of water. These findings suggest a significant transfer of electron density from the coordinating water molecule to the CPO-27-Zn framework. In the monohydrate framework, this creates a positive net charge (+0.105) on the coordinating water molecule. Addition of more, non-coordinating water molecules, gradually reduces this net charge through H-bonding.[63] For 50% and 70% hydration ($Zn_2(dobdc)(H_2O)_5$, $Zn_2(dobdc)(H_2O)_7$, obtained by MD simulation), the net charge of the coordinating molecule is reduced to 0.071 and 0.051, respectively. In turn, a positively charged layer in the non-coordinating water domain is observed at a distance between *ca.* 3 and 5 Å from the pore center. However, we do not observe the creation of a negatively charged sublayer or significant changes in charges of all hydrogen atoms (Figures S2 and S3, Supporting Information). We note that our observations stand in slight contrast to previous DFT calculations on gas-phase fragments of desolvated CPO-27-*M*,[34] where higher charges for all atoms as well as a higher charge for O_{Cp} than for O_P were observed, contrary to our results. We attribute these differences to the different approach and applied methods (here: continuous framework) and to deviating degrees of pore filling.

CPO-27-Cu shows an entirely different picture, consistent with our experimental findings. After hydration and geometric relaxation, the local Cu environment undergoes a radical change from a distorted square-pyramidal to a highly distorted, nearly square-planar configuration (Figure 5d/f). This is a consequence of the elongation of the axial Cu—O_{Ci} bond from 2.42 to 2.60 Å (as the Cu center moves into the direction of the pore space) and the low affinity of the Cu center to water resulting in a large Cu—O_{water} distance of 2.64 Å (for the closest water molecule). Both axial bonds are *ca.* 0.2 Å longer than for the loosely bound axial water molecules in the hexaaqua copper(II) complex,[64-66] which is right at the boundary of the combined van-der-Waals radii.[67] Additionally, the water molecule is tilted toward the equatorial CuO_4 plane (bond lengths of 1.99 ± 0.02 Å) with one hydrogen atom pointing toward the O_{Cp} and O_P atoms, highlighted by two short O_{MOF}—H_{water} distances below 2.5 Å (see Table S3, Supporting Information). These observations verify our previously mentioned assumption that water does not coordinate to the open Cu metal site and instead interacts with the O atoms of the inorganic building unit via H-bonding.

Upon hydration, the atomic charge of the Cu center increases notably; for 20% hydration ($Cu_2(dobdc)(H_2O)_2$), the charge becomes less positive (+0.873 → +0.840, see Table S5, Supporting Information). Further, charges of O_P increase (−0.537 → −0.532) while the opposite is observed for O_{Cp} (−0.508 → −0.522). At the O_{Ci} atom, the charge also decreases (−0.601 → −0.587), with its negative charge remaining the highest observed. For 50% hydration ($Cu_2(dobdc)(H_2O)_5$, obtained by MD simulation), remarkably similar values are observed, which confirms that the impact of the first water molecule can hardly be distinguished from additional ones. Interestingly, we observe a broadening of the standard deviation for all oxygen atoms, which seems to depend on their accessibility to form H-bonds ($O_{Cp} > O_P > O_{Ci}$).[63] In addition, we observe a minor intra-molecular electron density transfer from the O to the H atoms, which is more pronounced for water molecules near the framework atoms, but does not affect the charge balance in water (Figure S4, Supporting Information). In contrast to previous experiments on water surfaces,[63] no (positively or negatively) charged sub-surfaces are observed in our study, which we attribute to (i) the confined space, as the reported depths for negatively charged subsurface layers lay between 3 and 8 Å,[63] and (ii) the limited interactions of the framework atoms with the confined water molecules. Except for the already mentioned significantly higher charges in previous DFT calculations,[34] we observe the same trends in our calculations on CPO-27-Cu.

In summary, the DFT data confirm significantly different situations for CPO-27-Zn and CPO-27-Cu (Figure 5g). Coordination of water to the open metal site in CPO-27-Zn results in a slightly distorted octahedral coordination environment of the Zn center, which becomes more positive in charge. Further, the more approachable O_{Cp} atoms possess the highest negative charge of all O atoms, thus favoring H-bonding with water, acting as secondary sorption sites. Otherwise, minor changes to the local Zn environment are observed. CPO-27-Cu shows a more drastic change. As a result of the higher electron densities of Cu and O_{Ci} after hydration, the Cu–O_{Ci} distance is strongly elongated, suggesting that O_{Ci} leaves the Cu coordination sphere. Further, no water molecules are in close proximity to the Cu center as water molecules interact with the O atoms of the framework (O_{Cp} and O_P) via H-bonding. As a consequence, the previously square-pyramidal environment of the Cu center is transformed to nearly square-planar geometry.

Next, we studied the spatial distribution of water molecules in the pores of CPO-27-Zn and CPO-27-Cu for different degrees of pore filling by molecular dynamics simulation. For CPO-27-Zn, the stepwise water uptake in the vapor sorption isotherm (Figure 4) suggests that the water molecules occupy defined, individual sites within the pores, similar to what crystallographic data revealed.[25] Addition of the first water molecule per Zn (*i.e.* $Zn_2(dobdc)(H_2O)_2$, monohydrate material) results in the saturation of the first site, which is the open metal site, as shown in the H_2O density probability histogram (**Figure 6a**). In the water sorption isotherm (Figure 4), this corresponds to the first, irreversible adsorption step (20% total water uptake). In the radial O_{water} density distribution (Figure S5, Supporting Information), this corresponds to the single, narrow peak at 5.5 Å distance from the pore center. We note that the coordinating water molecules show only slight vibrational displacement.

Addition of another *ca.* 1.5 water molecules per Zn (*i.e.* $Zn_2(dobdc)(H_2O)_5$) results in a weighted O occupancy of the other four sites. These are located at distances (from the pore center) of 5.5 Å (second site, same distance as the first site, compare

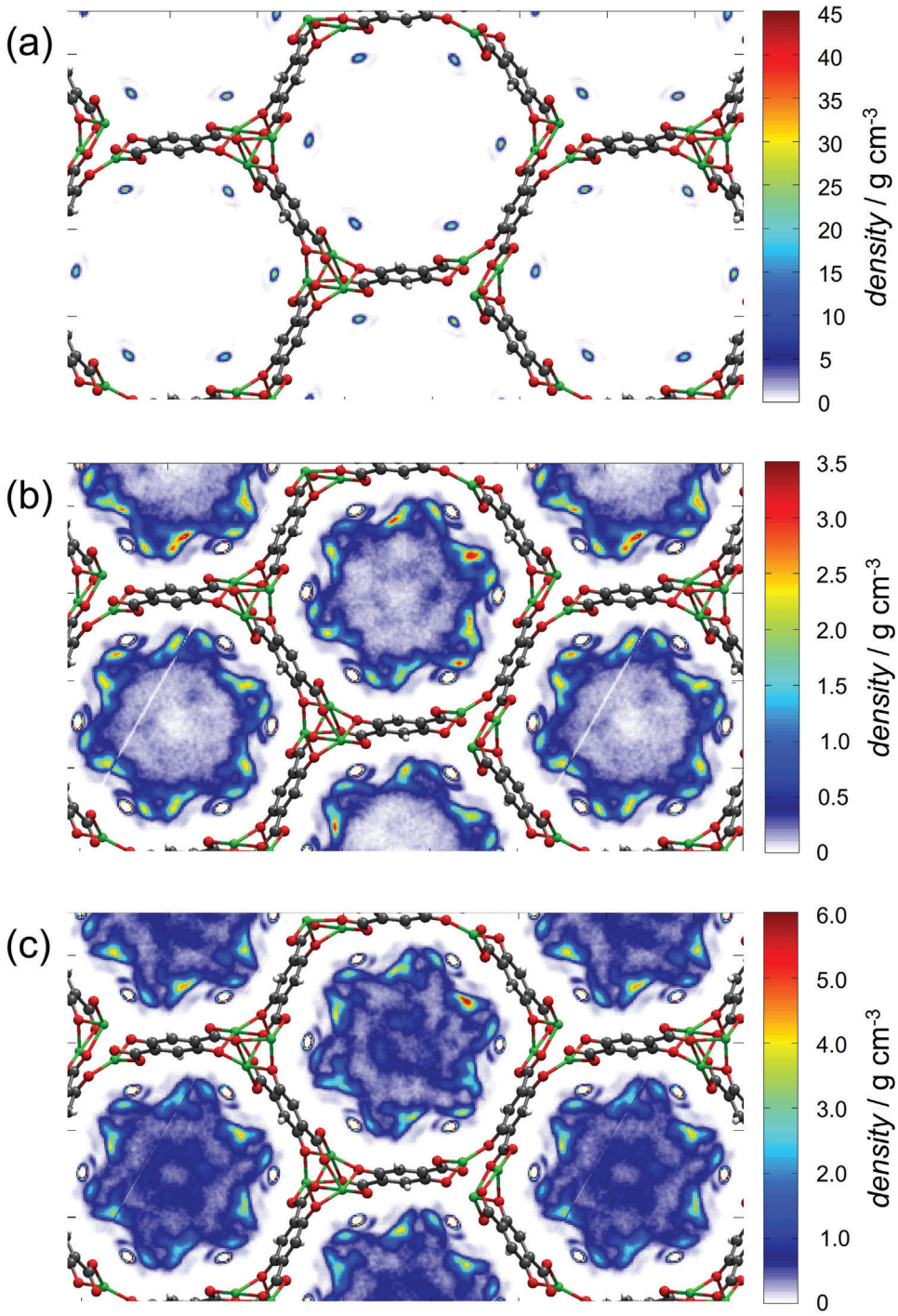

Figure 6. Probability density distribution histograms of water in CPO-27-Zn = $Zn_2(dobdc)(H_2O)_x$; (a) $x = 2$ (monohydrate), (b) $x = 5$, and (c) $x = 7$. For clarity, values > 3.5 and > 6.0 g cm^{-3} (occurring at the coordinating water molecule) are not shown in images (b) and (c), respectively; histograms with the full density value range are shown in Figure S7 (Supporting Information). (White lines are due to periodic boundary conditions of our simulations. Missing bonds in the framework structure are an artefact of the used VMD software package and do not refer to the real connectivity between the framework atoms. Unusually high densities stem from the small grid, that is, < 0.1 × 0.1 Å^2, that was used to track the position of the atomic nuclei, used for density calculations.).

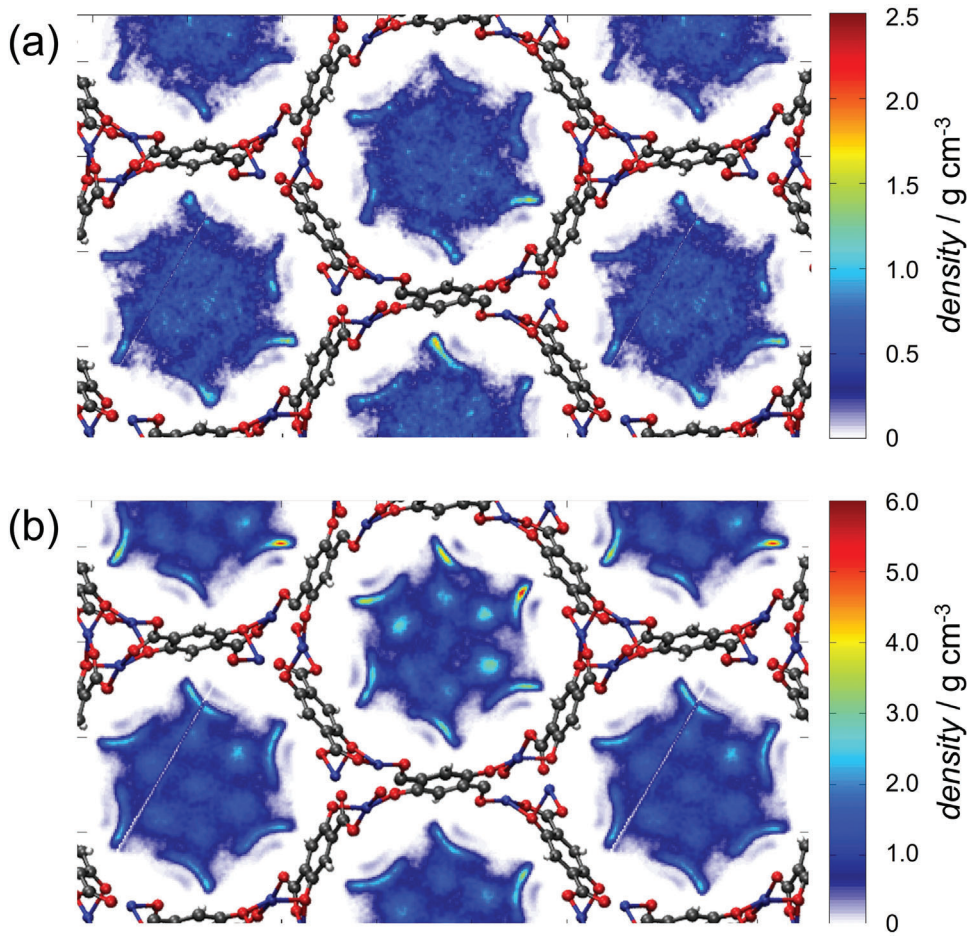

Figure 7. Probability density distribution histograms of water in CPO-27-Cu = $Cu_2(dobdc)(H_2O)_x$, (a) $x = 2$ (monohydrate) and (b) $x = 5$. Molecules form a star-like structure, resulting in seven pillars in the pore center. No molecules are found close to Cu, creating an empty space in its vicinity. Water shows a clear preference for H-bond formation with the framework carboxylate O atoms.

Figure S6, Supporting Information), 4.85 Å (third site), 4.05 Å (fourth site), and 1.3 Å (fifth site) (Figures S5 and S6, Supporting Information). This is supported by the density probability histogram (Figure 6b) that shows high occupancies at the second, third, and fourth site, because of the previously described H-bonding to framework oxygen atoms (O_{Cp} and O_P, see also H_{water} atom distribution, Figure S8, Supporting Information). The non-coordinating water molecules (*i.e.* second to fifth site) are 'mobile', that is, they exchange between sites,[35] resulting in broad density distributions along preferred paths. Negligible oxygen density is found near the center of the pore (fifth site), which makes it virtually indistinguishable from random movement through the pore. Again, this is consistent with the water sorption isotherms.

Further addition of another water molecule per Zn (*i.e.* $Zn_2(dobdc)(H_2O)_7$) increases the population of all available positions (Figure 6c). Those near the pore center experience the largest growth in occupancy (fourth and fifth adsorption site). In addition, the H_{water} atom distribution (Figure S8, Supporting Information) shows a strong preference for the added water molecules toward the pore center, resulting in the connection of all oxygen atoms via a H-bond network. This aligns with the third step in the water sorption isotherm (Figure 4a), expecting a preliminary pore saturation (*i.e.*, meta-stable state). We hypothesize that further addition of water to the framework will result in more distinct positions, matching those found in previous hydration experiments.[9] This is a gradual process that slowly progresses over a larger relative water pressure range as the movement of water molecules between different sorption sites becomes severely more hindered with each adsorbed water molecule. This is what the water sorption data (Figure 4a) suggest; future work will be dedicated to confirm this hypothesis by molecular dynamics simulation. We note that our radial water densities in CPO-27-Zn matches the general trend previously reported for CPO-27-Mg.[36] However, we observe a different weighting of the individual peaks, which may stem from (i) the incomplete pore filling in our system and/or (ii) the different metals discussed and/or (iii) the different methods used.

For CPO-27-Cu, addition of the first water molecule per Cu center (*i.e.* $Cu_2(dobdc)(H_2O)_2$, monohydrate material) does not suggest occupation of the open metal site (**Figure** 7a), consistent with the above-made observations. Rather, the water molecules

tend to reside at the center of the pore (see also Figure S5, Supporting Information). We note that this state is not observed in the water sorption measurement, since adsorption of the first *ca.* 80% water occurs nearly simultaneously (Figure 4). Addition of another *ca.* 1.5 water molecules per Cu (*i.e.* $Cu_2(dobdc)(H_2O)_5$, Figure 7b) allows a more conclusive view on the interactions and arrangement of the water molecules, even though it marks a transition state during the sole sorption step in our experiments. As stated above, no oxygen atoms are found in proximity to the Cu center, resulting in an empty pocket. The nearest water molecules form H-bonds toward the O_P and O_{Cp} atoms, while others form additional H-bonds toward the O_{Cp} atoms. This eventually enforces a curved, star-like water arrangement (Figure S9b, Supporting Information). The pronounced peak in the radial density plots centered at 4.0 Å (see Figure S5, Supporting Information) indicates the accumulation of water close to the phenylene ring (third sorption site), which matches our findings on CPO-27-Zn and previous findings on CPO-27-Mg.[36] Close to the center of the pore, no preferred hydrogen atom orientations or positions are visible (Figure S9, Supporting Information). We observe the formation of seven pillar-like water clusters along the channel axis, one of which is located in the exact center of the pore (peaks at 2.5 and 0 Å, respectively, see Figure S5, Supporting Information). We assume that at higher loadings, the visible arrangement becomes more pronounced, as our results suggest that the perpendicular water clusters increase in intensity with water uptake. As soon as enough water molecules can be adsorbed (*ca.* 80% of total uptake with respect to our sorption experiments), accumulation of the aforementioned interactions results in pore condensation.

In summary, the molecular dynamics simulations confirm that water shows much stronger affinity to the open metal site in CPO-27-Zn than in CPO-27-Cu. As a result, the mechanism of pore filling and the structure of water in the filled pore are entirely different.

3. Conclusion

By combining experimental methods (manometric water vapor sorption analysis and FTIR spectroscopy) with DFT and MD calculations, we were able to obtain a comprehensive picture of the uptake of water in CPO-27-Zn and CPO-27-Cu. This includes the distinction of individual sorption sites and water-induced structural relaxation of the frameworks. CPO-27-Zn and CPO-27-Cu, though topologically identical, show completely different properties with respect to hydration. The uptake of water into the micropores occurs via different mechanisms, and the resulting structure of the water in the pores is also different. In CPO-27-Zn, water first coordinates to the Zn center. The coordinated water molecule serves as an anchor for adsorption of further water molecules by H-bonding, although the latter also form H-bonds with framework oxygen atoms. Adsorption occurs stepwise, with water molecules occupying defined positions inside the pores and exchanging between them. In CPO-27-Cu, water does not coordinate to the metal center for geometric reasons and for resulting electron density distribution; the respective position remains unoccupied. Water molecules adsorb to the pore wall by H-bonding to framework oxygen atoms. Pore filling occurs all at once, like classical pore condensation. Water in the pores of CPO-27-Cu show high mobility, forming clusters along the pore axis. The DFT as well as the MD calculations validate the distinct difference in behavior in the two CPO-27 materials. We have shown that the water in CPO-27-Zn accumulates at defined positions. The strength of interaction depends on the position inside the cell and relates to the electronic interactions between the framework and water molecules, which favor a step-wise pore condensation process. For CPO-27-Cu we observe a distinct difference in both structure and electronic interactions in the simulations. We found little interactions between MOF and water, which favor a complete pore condensation in one step.

Supporting Information

Supporting Information is available from the Wiley Online Library or from the author.

Acknowledgements

The generous allocation of computing time on the supercomputer "Noctua2" by the Paderborn Center for Parallel Computing (PC2) is kindly acknowledged.

Open access funding enabled and organized by Projekt DEAL.

Conflict of Interest

The authors declare no conflict of interest.

Data Availability Statement

The data that support the findings of this study are available in the supplementary material of this article.

Keywords

CPO-27, DFT calculations, metal-organic frameworks, MOF-74, molecular dynamics, open metal sites, water vapor sorption

Received: May 30, 2024
Revised: July 25, 2024
Published online:

[1] C. Janiak, J. K. Vieth, *New J. Chem.* **2010**, *34*, 2366.
[2] R. Freund, O. Zaremba, G. Arnauts, R. Ameloot, G. Skorupskii, M. Dinca, A. Bavykina, J. Gascon, A. Ejsmont, J. Goscianska, M. Kalmutzki, U. Lächelt, E. Ploetz, C. S. Diercks, S. Wuttke, *Angew. Chem., Int. Ed.* **2021**, *60*, 23975.
[3] Ü. Kökçam-Demir, A. Goldman, L. Esrafili, M. Gharib, A. Morsali, O. Weingart, C. Janiak, *Chem. Soc. Rev.* **2020**, *49*, 2751.
[4] P. D. C. Dietzel, Y. Morita, R. Blom, H. Fjellvåg, *Angew. Chem., Int. Ed.* **2005**, *44*, 6354.
[5] N. L. Rosi, J. Kim, M. Eddaoudi, B. Chen, M. O'Keeffe, O. M. Yaghi, *J. Am. Chem. Soc.* **2005**, *127*, 1504.
[6] G. Calleja, R. Sanz, G. Orcajo, D. Briones, P. Leo, F. Martínez, *Catal. Today.* **2014**, *227*, 130.
[7] E. O. Fetisov, M. S. Shah, J. R. Long, M. Tsapatsis, J. I. Siepmann, *Chem. Commun.* **2018**, *54*, 10816.

[8] I. Strauss, A. Mundstock, D. Hinrichs, R. Himstedt, A. Knebel, C. Reinhardt, D. Dorfs, J. Caro, *Angew. Chem., Int. Ed.* **2018**, *57*, 7434.
[9] M. H. Rosnes, B. Pato-Doldán, R. E. Johnsen, A. Mundstock, J. Caro, P. D. C. Dietzel, *Microp. Mesop. Mater.* **2020**, *309*, 110503.
[10] L. J. Small, M. E. Schindelholz, T. M. Nenoff, *Ind. Eng. Chem. Res.* **2021**, *60*, 7998.
[11] J. Yan, J. Feng, J. Ge, J. Chen, F. Wang, C. Xiang, D. Wang, Q. Yu, H. Zeng, *IEEE Photonics Technol. Lett.* **2022**, *34*, 77.
[12] M. J. Kalmutzki, C. S. Diercks, O. M. Yaghi, *Adv. Mater.* **2018**, *30*, 1704304.
[13] N. Hanikel, M. S. Prévot, O. M. Yaghi, *Nat. Nanotechnol.* **2020**, *15*, 348.
[14] C. Solís, D. Palaci, F. X. Llabres i Xamena, J. M. Serra, *J. Phys. Chem. C.* **2014**, *118*, 21663.
[15] S. Hwang, E. J. Lee, D. Song, N. C. Jeong, *ACS Appl. Mater. Interfaces.* **2018**, *10*, 35354.
[16] A. Javed, I. Strauss, H. Bunzen, J. Caro, M. Tiemann, *Nanomaterials.* **2020**, *10*, 1263.
[17] I. E. Khalil, J. Fonseca, M. R. Reithofer, T. Eder, J. M. Chin, *Coord. Chem. Rev.* **2023**, *481*, 215043.
[18] Y. R. Liu, Y. Y. Chen, H. Y. Zhao, G. Li, *Coord. Chem. Rev.* **2024**, *499*, 215516.
[19] M. F. Lange, K. J. F. M. Verouden, T. J. H. Vlugt, J. Gascon, F. Kapteijn, *Chem. Rev.* **2015**, *115*, 12205.
[20] I. Strauss, A. Mundstock, M. Treger, K. Lange, S. Hwang, C. Chmelik, P. Rusch, N. C. Bigall, T. Pichler, H. Shiozawa, J. Caro, *ACS Appl. Mater. Interfaces.* **2019**, *11*, 14175.
[21] L. T. Zhang, Y. Zhou, S. T. Han, *Angew. Chem., Int. Ed.* **2021**, *60*, 15192.
[22] T. M. McDonald, W. R. Lee, J. A. Mason, B. M. Wiers, C. S. Hong, J. R. Long, *J. Am. Chem. Soc.* **2012**, *134*, 7056.
[23] C. A. Trickett, A. Helal, B. A. Al-Maythalony, Z. H. Yamani, K. E. Cordova, O. M. Yaghi, *Nat. Rev. Mater.* **2017**, *2*, 17045.
[24] Y. S. Wei, M. Zhang, R. Zou, Q. Xu, *Chem. Rev.* **2020**, *120*, 12089.
[25] P. D. C. Dietzel, R. E. Johnsen, R. Blom, H. Fjellvåg, *Chem. - Eur. J.* **2008**, *14*, 2389.
[26] H. Furukawa, F. Gándara, Y. B. Zhang, J. Jiang, W. L. Queen, M. R. Hudson, O. M. Yaghi, *J. Am. Chem. Soc.* **2014**, *136*, 5271.
[27] B. Zhang, Z. Zhu, X. Wang, X. Liu, F. Kapteijn, *Adv. Funct. Mater.* **2023**, 2304788.
[28] J. B. DeCoste, G. W. Peterson, B. J. Schindler, K. L. Killops, M. A. Browe, J. J. Mahle, *J. Mater. Chem. A.* **2013**, *1*, 11922.
[29] P. M. Schoenecker, C. G. Carson, H. Jasuja, C. J. J. Flemming, K. S. Walton, *Ind. Eng. Chem. Res.* **2012**, *51*, 6513.
[30] A. Metrane, A. Delhali, M. Ouikhalfan, A. H. Assen, Y. Belmabkhout, *J. Chem. Eng. Data.* **2022**, *67*, 1617.
[31] C. Weinberger, F. Zysk, M. Hartmann, N. K. Kaliannan, W. Keil, T. D. Kühne, M. Tiemann, *Adv. Mater. Interfaces.* **2022**, *9*, 2200245.
[32] K. Lee, J. D. Howe, L.-C. Lin, B. Smit, J. B. Neaton, *Chem. Mater.* **2015**, *27*, 668.
[33] L. Valenzano, B. Civalleri, S. Chavan, G. T. Palomino, C. O. Areán, S. Bordiga, *J. Phys. Chem. C.* **2010**, *114*, 11185.
[34] T. Pham, K. A. Forrest, J. Eckert, B. Space, *Cryst. Growth Des.* **2016**, *16*, 867.
[35] Y. Li, X. Wang, D. Xu, J. D. Chung, M. Kaviany, B. Huang, *J. Phys. Chem. C.* **2015**, *119*, 13021.
[36] X. Peng, L. Lin, W. Sun, B. Smit, *AIChE J.* **2015**, *61*, 3708.
[37] M. G. Lopez, P. Canepa, T. Thonhauser, *J. Chem. Phys.* **2013**, *138*, 154704.
[38] T. A. Manz, N. G. Limas, *RSC Adv.* **2016**, *6*, 47771.
[39] N. G. Limas, T. A. Manz, *RSC Adv.* **2016**, *6*, 45727.
[40] T. A. Manz, D. S. Sholl, *J. Chem. Theory Comput.* **2010**, *6*, 2455.
[41] T. A. Manz, D. S. Sholl, *J. Chem. Theory Comput.* **2011**, *7*, 4146.
[42] T. A. Manz, D. S. Sholl, *J. Chem. Theory Comput.* **2012**, *8*, 2844.
[43] T. A. Manz, *RSC Adv.* **2017**, *7*, 45552.
[44] L. J. Wang, H. Deng, H. Furukawa, F. Gándara, K. E. Cordova, D. Peri, O. M. Yaghi, *Inorg. Chem.* **2014**, *53*, 10937.
[45] M. H. Rosnes, M. Opitz, M. Frontzek, W. Lohstroh, J. P. Embs, P. A. Georgiev, P. D. C. Dietzel, *J. Mater. Chem. A.* **2015**, *3*, 4827.
[46] M. Thommes, K. Kaneko, A. V. Neimark, J. P. Olivier, F. Rodriguez-Reinoso, J. Rouquerol, K. S. W. Sing, *Pure Appl. Chem.* **2015**, *87*, 1051.
[47] B. Pato-Doldán, M. H. Rosnes, P. D. C. Dietzel, *ChemSusChem.* **2017**, *10*, 1710.
[48] M. V. Veidis, G. H. Schreiber, T. E. Gough, G. J. Palenik, *J. Am. Chem. Soc.* **1969**, *91*, 1859.
[49] N. Heidary, D. Chartrand, A. Guiet, N. Kornienko, *Chem. Sci.* **2021**, *12*, 7324.
[50] G. Onori, A. Santucci, *J. Phys. Chem.* **1993**, *97*, 5430.
[51] T. Iiyama, M. Ruike, K. Kaneko, *Chem. Phys. Lett.* **2000**, *331*, 359.
[52] J. Alcañiz-Monge, A. Linares-Solano, B. Rand, *J. Phys. Chem. B.* **2002**, *106*, 3209.
[53] I. Brovchenko, A. Geiger, A. Oleinikova, *J. Phys. Condens. Matter.* **2004**, *16*, S5345.
[54] T. Ohba, H. Kanoh, K. Kaneko, *J. Phys. Chem. B.* **2004**, *108*, 14964.
[55] T. Ohba, H. Kanoh, K. Kaneko, *Nano Lett.* **2005**, *5*, 227.
[56] P. Gallo, M. Rovere, S.-H. Chen, *J. Phys. Condens. Matter.* **2010**, *22*, 284102.
[57] M. Sadeghi, G. A. Parsafar, *Phys. Chem. Chem. Phys.* **2013**, *15*, 7379.
[58] M. Thommes, J. Morell, K. A. Cychosz, M. Fröba, *Langmuir.* **2013**, *29*, 14893.
[59] J. B. Mietner, F. J. Brieler, Y. J. Lee, M. Fröba, *Angew. Chem., Int. Ed.* **2017**, *56*, 12348.
[60] B. Malfait, A. Moréac, A. Jani, R. Lefort, P. Huber, M. Fröba, D. Morineau, *J. Phys. Chem. C.* **2022**, *126*, 3520.
[61] K. Schlichte, T. Kratzke, S. Kaskel, *Microporous Mesoporous Mater.* **2004**, *73*, 81.
[62] M. Hartmann, T. Clark, R. van Eldik, *J. Am. Chem. Soc.* **1997**, *119*, 7843.
[63] R. Vàcha, O. Marsalek, A. P. Willard, D. J. Bonthuis, R. R. Netz, P. Jungwirth, *J. Phys. Chem. Lett.* **2012**, *3*, 107.
[64] T. K. Sham, J. B. Hastings, M. L. Perlman, *J. Am. Chem. Soc.* **1980**, *102*, 5904.
[65] A. Pasquarello, I. Petri, P. S. Salmon, O. Parisel, R. Car, É. Tóth, D. H. Powell, H. E. Fischer, L. Helm, A. E. Merbach, *Science.* **2001**, *291*, 856.
[66] S. Gómez-Salces, F. Aguado, R. Valiente, F. Rodríguez, *Angew. Chem., Int. Ed.* **2012**, *51*, 9335.
[67] A. Bondi, *J. Phys. Chem.* **1964**, *68*, 441.